JOURNAL OF SOLID STATE CHEMISTRY 57, 2–16 (1985)

Empty, Filled, and Condensed Metal Clusters*

ARNDT SIMON

Max-Planck-Institut fuer Festkoerperforschung, Heisenbergstrasse 1, 7000-Stuttgart 80, Federal Republic of Germany

Received August 13, 1984

Aspects of structure, bonding, physical, and chemical properties are discussed for (a) compounds containing discrete empty clusters and clusters with interstitial H atoms: Nb_6I_{11}, HNb_6I_{11}, $HCsNb_6I_{11}$, (b) metal-rich lanthanide halides and halide carbides, –nitrides and –hydrides, focusing on the role of interstitial atoms: $Gd_2Br_2C_2$, Gd_2Br_2C, Gd_3Cl_3C, $Gd_{10}Cl_{18}C_4$, $Gd_{10}Cl_{17}C_4$, $Gd_{10}I_{16}C_4$, Gd_2Cl_3N, $GdXH_n$ (X = Cl, Br, I; $0.6 < n < 0.9$), $GdBrD_2$; (c) metal-rich oxides of the alkali metals rubidium and cesium. Chemical bonding in the suboxide clusters Rb_9O_2 and $Cs_{11}O_3$ is discussed along the lines valid for (a) and (b) and covers recently described "hypervalent" species as Li_6C, Li_4O, etc.

Introduction

Metal cluster chemistry has developed remarkably in the last 20 years. There exists multiple bonding not accessible to main group elements (*1*), and there exist unique physical properties, as observed with the "Chevrel" compounds (*2*). But it seems even more important that different directions of chemistry meet in the field of metal clusters. "Molecular chemists" prepare larger and larger clusters, like Pt_n (n = 19, 24, 38, . . .) (*3, 4*) or Au_{55} clusters (*5*), thus entering the gap between the discrete molecule and the infinite solid, as "solid-state chemists" discuss typical solid-state structures in terms of molecular entities (*6–8*) and try to cut infinitely extended cluster structures into finite pieces. Besides much experimentation and empirical approaches the growing interest in a quantitative treatise of chemical bonding including extended cluster structures is obvious (*9–17*), i.e., different chemical approaches and the physicists' view of structure are combined.

Talking about filled clusters calls for a cavity; discussion will be restricted to units with octahedral M_6 cores. On the basis of filling such clusters with nonmetal atoms and of condensing them, a somewhat unified view of cluster formation with quite different metals—*d* metals, lanthanides, and even alkali metals—is presented. Metal-rich compounds of metals which have only few valence electrons clearly reveal the borderline between cluster compounds with metal–metal bonding and conventional valence compounds where structures with cluster-like units occur due to strong metal–nonmetal bonding.

---

* Presented at the Symposium on Metal–Metal Bonding in Solid State Clusters and Extended Arrays, held during the American Chemical Society meeting, St. Louis, Missouri, April 9–10, 1984.

0022-4596/85 $3.00

Electron-Deficient Clusters

Clusters of the M_6X_8 and M_6X_{12} types frequently occur with *d* metals of groups 4 to 7. The first is favored with a high *d*-electron concentration (22, 24, 30) (*18*), the latter with up to 16 *d* electrons per M_6 unit available for metal–metal bonding. Compounds with less than these "magic" numbers of electrons offer fascinating chemical as well as physical properties. Compounds containing the Nb_6I_8 cluster might serve as an example.

Investigations on Nb_6I_{11} (= $Nb_6I_8I_{6/2}$) have been described in detail elsewhere (*19–27*) so here only those aspects are briefly discussed and attention is drawn to those original papers which (a) give insight into the intimate relations between chemical and physical properties of this compound which both belong to it in the same way as front and back belong to a coin, (b) provide a feeling for the degree of quantitative understanding reached with *d* metal clusters, and last but not least, (c) provide qualitative arguments for an understanding of the cluster chemistry of the electron-poor metals of groups 3 and 4. In spite of having only ($6 \times 5 - 11 =$) 19 *d* electrons for Nb–Nb bonds the compound Nb_6I_{11} chooses to form the Nb_6I_8 cluster at the expense of electron deficiency and lattice instability, and these two consequences are clearly reflected in the compound properties: (i) chemistry: topochemical reaction with amines.

(ii) physics: spin-crossover transition.

(i) With amines (RNH_2; e.g., R = H, CH_3, C_3H_7) a crystal of Nb_6I_{11} breaks up into very thin lamellae within seconds. The amine first attacks the most strained I bridges between layers of interconnected clusters. After some days, compounds of composition $Nb_6I_8(RNH_2)_6$ are formed (*27*). The reaction with amine thus takes the strain from the framework of interconnected Nb_6I_8 clusters in Nb_6I_{11} and adds electrons to the cluster via a redox reaction. The cluster in $Nb_6I_8(RNH_2)_6$ contains 22 electrons; a part of the Nb_6I_{11} is oxidized to an amorphous solid. Having in mind the interesting properties of compounds containing bare Mo_6X_8 clusters (X = S, Se, Te), a compound with bare Nb_6I_8 clusters should be important. Until now we were not able to cleave off the neutral amine ligands without decomposition of the cluster. Heating the compound under vacuum leads to a loss of only four of the six ligands, and unfortunately the residue is amorphous and nonmetallic. $Nb_6I_8(RNH_2)_6$ contains Nb_6I_8 clusters in the lowest oxidation state known. Experiments to form a compound which is isotypic with $Li_4Re_6S_{11}$ (*28*)—an intercalate of Li atoms into a framework of the Nb_6I_{11} type—again were not successful, possibly due to size effects.

(ii) Nb_6I_{11} undergoes a phase transition at 274 K. The relation between high- and low-temperature forms fulfills Landau's criteria (*Pccn* → *P*2₁*cn*) for a second-order transition (*25*). The transition occurs due to a lattice instability clearly involving the inter-

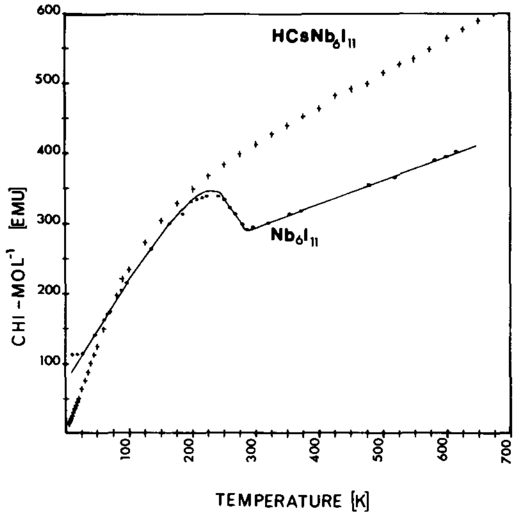

FIG. 1. Inverse magnetic susceptibilities of Nb_6I_{11} and $HCsNb_6I_{11}$ showing doublet–quartet transitions which occur smoothly with $HCsNb_6I_{11}$ and are accompanied by a structural phase transition with Nb_6I_{11}.

connecting I bridges as well as due to the electron deficiency of the cluster. The structural feature of the transition is a twist deformation of the M_6 unit relative to one of its quasitrigonal axes accompanied by a loss of the inversion center. This deformation is assisted by the very anisotropic vibrations of the interconnecting I atoms. The energetic feature of the transition is a close approach of HOMO's and LUMO's with increasing temperature leading to a decoupling of an electron pair and a change from a doublet to a quartet ground state (*22, 23*). However, the energy gain due to this "spin-crossover"—the first observed for a metal cluster compound—cannot be the driving force for the phase transition. In fact the large entropy change in the transition indicates significant vibrational changes, most probably connected with a soft-mode behavior of the interconnecting iodine and the niobium atoms.

With respect to the lattice instability it is interesting to compare the behavior of Nb_6I_{11} with that of a compound which allows the characteristic twist deformation of the Nb_6I_8 cluster without the necessity of symmetry breaking. $CsNb_6I_{11}$ (*29*) can be made an odd-electron system by incorporating hydrogen (*29*), and the compound $CsNb_6I_{11}H$ shows essentially the same spin-crossover as Nb_6I_{11} (Fig. 1). But as the Cs compound is trigonal, the twist deformation of the cluster occurs continuously within space group $P6_322$, and consequently a smooth change of the magnetic moment is observed as a function of temperature (*30*).

Filled and Condensed Metal Clusters

Nb_6I_{11} absorbs hydrogen to form $Nb_6I_{11}H$ (*21*). It becomes nonmagnetic at low temperature and the phase transition, now accompanied by a change from a singlet to triplet state, is shifted to 324 K. Except for the structural transition this behavior is similar to that of $CsNb_6I_{11}$ (*30*) which must be formulated as $Cs^+Nb_6I_{11}^-$. Hydrogen therefore adds an electron to the Nb_6I_8 cluster in $Nb_6I_{11}H$. The electron number in $CsNb_6I_{11}$, too, can be increased by one in $CsNb_6I_{11}H$ (*29*) changing the compound to paramagnetic also at low temperature as discussed in the last section. Superficially, both Cs and H act as electron donors, yet their function is quite different. The external Cs atom simply adds its electron into a bonding cluster state, whereas the H atom, incorporated in the central cavity of the cluster, increases the total number of electrons but still strongly participates in them. The interpretation of the bonding as given before (*26, 31*) will not change in its essential parts even when the H atom is slightly displaced from the central cluster position (*32*). According to this interpretation the introduction of a hydrogen atom into the cluster does not change the number of bonding states but only changes their relative energies. In essence, cluster stabilization comes from a strongly bonding state with mainly hydrogen character. The bonding of hydrogen atoms in the metallic hydrides, e.g., in PdH_x and NiH_x is explained in a similar way (*33, 34*). Here, the metal–hydrogen bonding states essentially come from low-lying filled band states of the metal which can overlap with the *s* orbital of the H atoms and the added electrons fill band holes at the Fermi level. A similar bond picture holds for carbides (*35, 36*).

To summarize the consequence: Electron-deficient metal clusters gain stability by incorporating nonmetal atoms. This reduces (peripheral) metal–metal bond strength but builds up strong central metal–nonmetal bonds. The extreme of this view might be compared to the inverse situation of a weakly bonded Cl_6 octahedron. Introduction of a W atom leads to the stable entity WCl_6 by opening all Cl–Cl bonds and forming strong W–Cl bonds (*37*).

M_6X_8 and M_6X_{12} clusters play an important role with halides of low-valent 4*d* and

$5d$ metals of groups 4 to 6. With Mo and especially Re the valence electron concentration is sufficiently hight to allow for the M_6X_8 cluster with the divalent chalcogens, too. It seems logical that the same type of cluster is formed with electron-poor transition metals and/or multivalent anions provided the metal-to-nonmetal ratio is large in the compound to yield a sufficiently high d-electron concentration for M–M bonding. As a consequence the nonmetal content might be so low that the clusters have to be condensed via M–M bonding. A large number of metal-rich compounds between d metals and p elements can in fact be discussed in terms of condensed M_6X_8 or M_6X_{12} clusters (*7*). Condensation occurs via corners, edges, and faces of the M_6 octahedron leading to metal–metal-bonded units of infinite extention. It is assuring to see evidence growing for the validity of such a qualitative concept both from the theoretical and experimental points of view.

Band-structure calculations for TiO and NbO (*15, 16*) are in agreement with the assumption of M–M bonds in frameworks of condensed M_6X_{12} clusters (*7, 38*). The band structure of the chain of corner-sharing octahedra in Ti_5Te_4-type compounds reveals a close relationship to the bonding in the isolated M_6X_8 cluster (*17, 39*); detailed band-structure calculations have also been performed for the edge-sharing case as in the anion $Mo_3S_3^-$ (*10–12, 14*). Tracing back the band structure to the bonds in a discrete M_6X_8 cluster is difficult here because the environment of the M_6 core in the isolated and condensed units (bond angles and the occupation of nonmetal positions) differ considerably. On the other hand, cluster condensation is reflected as chemical evidence in the field of ternary molybdenum chalcogenides, where a number of intermediates with general compositions $Mo_{3(n+1)}X_{3(n+1)+2}$ between the isolated Mo_6X_8 cluster and the infinite Mo_3X_3 chain have been synthesized recently (*40*). Besides the individual view, i.e., the condensation of quasimolecular units, the collective view is also in its right. Franzen (*41, 42*) has pointed out that the extended metal–metal-bonded parts in metal-rich compounds exhibit a local order as in the elements themselves. Band structures of such compounds should contain features of both the pure metal and the isolated cluster.

Clusters with Lanthanides

A series of metal-rich lanthanide halides varying in halogen-to-metal ratio $X/Ln < 2$ has been prepared and structurally characterized. All these phases contain octahedral Ln_6 units which are isolated for $X/Ln = 1.71$ and condensed into chains for $X/Ln = 1.60$, 1.50, 1.25, double chains for $X/Ln = 1.43$, 1.17, or layers for $X/Ln = 1.00$ (*7, 31, 43–54*). The arrangement of X atoms around the Ln_6 units is equivalent to that in the M_6X_8 and M_6X_{12} clusters.

Cluster condensation and cluster filling seem to be essential aspects in the structural chemistry of the valence-electron-poor lanthanides in their low oxidation states. Introduction of nonmetal atoms into the cavities of Ln_6 units is easily possible in many cases and, according to our present knowledge obviously frequently necessary to stabilize compounds with otherwise too weak metal–metal bonds.

The first such compound of the lanthanides with filled Ln_6 units was $Gd_{10}Cl_{18}C_4$. Its structure contains units of two edge-sharing Gd_6 octahedra surrounded by Cl atoms above all free edges and each octahedron containing a C_2 unit in its center (*55, 56*). By reaction of the metal, trihalide, and graphite a number of halide carbides could be prepared and characterized analytically and structurally, they are summarized in Table I. Some of these compounds are directly derived by introducing carbon into cavities in the earlier described structures of binary halides, e.g., $Gd_2Br_2C_2$,

TABLE I

GADOLINIUM HALIDE CARBIDES

Compound	Space group	Lattice constants [pm, °]			C_n d(C–C) [pm]	Framework	Ref.
$Gd_2Br_2C_2$	$C2/m$	$a = 702.5$	$b = 383.6$	$c = 986.8$	C_2 127	$(Gd_2Br_2)^{4+}$	(57)
			$\beta = 94.47$				
$Gd_{10}Cl_{18}C_4$	$P2_1/c$	$a = 918.2$	$b = 1612.0$	$c = 1288.6$	C_2 147	$(Gd_5Cl_9)^{6+}$	(56)
			$\beta = 119.86$				
$Gd_{12}I_{17}C_6$	$C2/c$	$a = 1929.7$	$b = 1220.1$	$c = 1863.5$	C_2 145	$(Gd_4I_{57})^{63+}$	(58)
			$\beta = 90.37$				
$Gd_{10}Cl_{17}C_4$	$P\bar{1}$	$a = 849.8$	$b = 917.4$	$c = 1146.2$	C_2 147	$(Gd_5Cl_9)^{65+}$	(56)
		$\alpha = 104.56$	$\beta = 95.98$	$\gamma = 111.35$			
$Gd_{10}I_{16}C_4$	$P\bar{1}$	$a = 1046.3$	$b = 1694.5$	$c = 1122.0$	C_2 143	$(Gd_5I_8)^{7+}$	(59)
		$\alpha = 99.15$	$\beta = 92.68$	$\gamma = 88.06$			
Gd_2Br_2C	$P\bar{3}m1$	$a = 382.09$		$c = 982.4$	C —	$(Gd_4Br_4)^{8+}$	(57)
$Gd_6Br_7C_2$	$C2/m$	$a = 2074.8$	$b = 381.9$	$c = 1188.5$	C —	$(Gd_6Br_7)^{11+}$	(57)
			$\beta = 124.73$				
$Gd_6I_7C_2$	$C2/m$	$a = 2137.5$	$b = 386.9$	$c = 1231.9$	C —	$(Gd_6I_7)^{11+}$	(59)
			$\beta = 123.5$				
Gd_3Cl_3C	$I4_132$	$a = 1073.4$			C —	$(Gd_6Cl_6)^{12+}$	(60)
Gd_4I_5C	$C2/m$	$a = 1858.7$	$b = 397.8$	$c = 856.1$	C —	$(Gd_8I_{10})^{14+}$	(59)
			$\beta = 103.26$				

Note. The positive charges of the Gd/X framework indicate how many electrons can be transferred to a C_2 unit.

Gd_2Br_2C or $Gd_6Br_7C_2$, Gd_4I_5C. Others contain structural frameworks which had not been observed earlier like $Gd_{12}I_{17}C_6$ or Gd_3Cl_3C. The most interesting feature with the lanthanide halide carbides is related to the fact that single C atoms as well as C_2 units with different C–C distances occur.

The type of carbon unit as well as the observed C–C distances are easily explained in terms of the number of electrons which can be transferred from the *Ln*/*X* framework to each C_2 unit. As a first approximation the C–C bonding is described on the basis of the simple *MO* pattern for a free C_2 unit. A discussion of selected compounds might be sufficient to illustrate these ideas and give some impression of chemical and physical consequences.

$Gd_2Br_2C_2$ (*57, 61*) crystallizes in gold-colored platelets with an analytically determined composition $Gd_{1.00}Br_{1.01}C_{0.98}$. The monoclinic structure contains $BrGdC_2GdBr$ slabs, one per repeat distance *c*. The stacking within the slabs corresponds to a sequence $Ab\gamma aB$ ($A, B \triangleq$ Br; $a, b \triangleq$ Gd; $\gamma = C_2$). It is identical with the stacking found in Sc_2Cl_2C (*62*) and different from that in the monohalide described as GdBr. Whereas the slabs in the latter compounds are constructed by condensing Gd_6Br_8 clusters—the Br atoms lie adjacent to the octahedral voids of the metal double layer—the slabs in $Gd_2Br_2C_2$ are derived from Gd_6Br_{12} clusters with Br atoms lying adjacent to tetrahedral voids. $Gd_2Br_2C_2$ shows a characteristic distortion of the layers from the trigonal symmetry of ZrCl and ZrBr (*63, 64*) and the corresponding carbon-free *Ln* halides. The loss of the threefold axis in $Gd_2Br_2C_2$ is easily rationalized from an inspection of Fig. 2 as caused by the special orientation of the C_2 units. The Gd atoms in "side-on" positions to the C_2 group exhibit Gd–Gd distances of 345 and 384 pm, whereas the "end-on" atoms have distances of 392 and 400 pm to the atoms in the

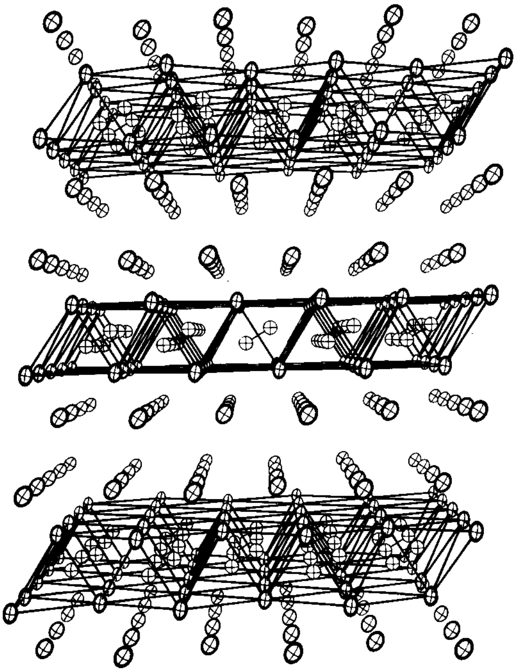

FIG. 2. Perspective drawing of the structure of $Gd_2Br_2C_2$ onto (010). The Gd_6 octahedra (centered by C_2 units) are indicated by lines.

basis of the octahedron; the distances parallel to the layers are the shorter ones. Only one mirror plane is preserved in the Gd_6 octahedron. The C–C distance is 127 pm and corresponds to a bond order between 2 and 3.

A bond order of two for the C–C bond is calculated, if it is assumed that the (ionic) framework $(Gd^{3+})_2(Br^-)_2$ provides 4 electrons per C_2 unit, filling all but two antibonding states. The relative shortening of the C–C double bond then might be due to a back-donation from antibonding carbon π^* states into empty d states of the metal atoms. The bonding in $Gd_2Br_2C_2$ is reflected in the chemical properties of the compound. Hydrolysis at room temperature yields mainly C_2 species, namely, C_2H_6 (69%), C_2H_4 (22%), C_2H_2 (4%), besides CH_4 (3%) but also C_4H_{10} (1%) and C_4H_8 (1-butene 1%, traces of *cis-* and *trans*-butene). The bond description is also in accordance with physical measurements. $Gd_2Br_2C_2$ shows very good electrical conductivity. The specific resistivity parallel to the layers is $\rho \approx 2.5 \cdot 10^{-4}\ \Omega$ cm. Below 30 K it decreases sharply, possibly related to the magnetic ordering which occurs. The ordering is reflected in a local minimum around 35 K and a maximum near 20 K in $1/\chi = f(T)$. It is interpreted in terms of canted antiferromagnetism (*61, 65*). The measurements can be accounted for by assuming ferromagnetic ordering within each Gd atom layer and nearly (deviation by 1°) antiparallel spins between layers.

Gd_2Br_2C (*57, 61*) forms bulky black graphite-like platelets. Its analytical composition is determined as $Gd_{1.00}Br_{0.96}C_{0.51}$. The compound crystallizes in a trigonal unit cell containing one slab BrGdCGdBr and the stacking of layers is derived from the Gd_6Br_{12} cluster as in $Gd_2Br_2C_2$. All investigated crystals are twinned. The structure had to be refined with the superimposed structure factor amplitudes of both crystals individually. It is noteworthy to mention that the C atoms in the structure, although their only sensible position is in the centers of Gd_6 octahedra, could not be identified by X rays. At a refinement level of $R = 0.074$ for the partial structure of the heavy atoms hardly any excess electron density is found.

Gd–Gd distances in Gd_2Br_2C differ markedly from those in tief-GdBr (ZrCl type) (*46*). The in-plane distances are 382 and 387 pm, respectively, and the distances between Gd atoms of adjacent planes are 343 and 357 pm. In spite of these differences the molar volumes (per Gd atom) are nearly the same in t-GdBr (38.0 $cm^3 \cdot mole^{-1}$) and Gd_2Br_2C (37.4 $cm^3 \cdot mole^{-1}$). Similar conditions hold for YCl and Y_2Cl_2C (33.4 and 32.8 $cm^3 \cdot mole^{-1}$, respectively) (*62*).

The occurrence of single C atoms (formally C^{4-} ions) in the structure of Gd_2Br_2C is again well understood in terms of the number of electrons provided by the framework of Gd and Br atoms. A C_2 unit cannot be stable in this compound, as there are 4 × 3 − 4 = 8 electrons per C_2 unit which is just sufficient to fill all antibonding states of the C_2 unit. As expected, the gaseous products of the hydrolysis of Gd_2Br_2C are distinctly different to those of $Gd_2Br_2C_2$. Main product is CH_4 (77%), but some C_2H_6 (18%), C_2H_4 (2%), and C_2H_2 (1.5%) are also found.

Figure 3 shows the projection of the structure of Gd_2Br_2C onto (11.0). Does the truth lie in between both representations?

Gd_3Cl_3C, though it seemingly represents only a compositional extention of the phases GdBrC, $GdBrC_{0.5}$ (→ $GdClC_{0.33}$), has a distinctly different crystal structure (*60*). It consists of a 3-dimensional framework of edge-sharing Gd octahedra centered by single C atoms and the halogen atoms lie above the edges of the octahedra. Chemical bonding, too, is different. Whereas $Gd_2Br_2C_2$ (assuming C–C double bonds) and Gd_2Br_2C are normal valence compounds according to the generalized (8 − *n*) rule (*66*), Gd_3Cl_3C is not. The electron concentration per C_2 unit (18 − 6 = 12) is high enough that all antibonding states of the C_2 unit are filled, thus rendering a molecular species unstable. But there are still more electrons which partially fill the metal *d* band. Gd_3Cl_3C naturally is a metal, whereas $Gd_2Br_2C_2$ and Gd_2Br_2C should be semiconductors. Their metallic properties come from electron delocalization due to an overlap of carbon *p* and metal *d* bands.

$Gd_{10}Cl_{18}C_4$, $Gd_{10}Cl_{17}C_4$, and $Gd_{10}I_{16}C_4$ form a family of compounds with closely related crystal structures. As shown in Fig. 4 the first compound contains isolated $Gd_{10}Cl_{18}C_4$ units (*56*). It is interesting to find a similar unit of two edge-sharing M_6 octahedra each centered by *one* C atom in the complex $Ru_{10}(CO)_{24}C_2$ (*67*). In $Gd_{10}Cl_{17}C_4$ two Cl atoms have a bridging function between adjacent clusters (*56*) and in $Gd_{10}I_{16}C_4$ four halogen atoms are bridging (*59*). Within standard deviations the C–C distances are identical in the three compounds, the value of approximately 145 pm corresponding to a slightly shortened C–C single bond. As in the case of $Gd_2Br_2C_2$ and Gd_2Br_2C the compound $Gd_{10}Cl_{18}C_4$ can be discussed as a normal valence compound. The (15 − 9 =) 6 electrons from the Gd/Cl framework are sufficient to fill all but the highest lying antibonding state of the C_2 unit. The slight shortening of the C–C distance might again be discussed in terms of

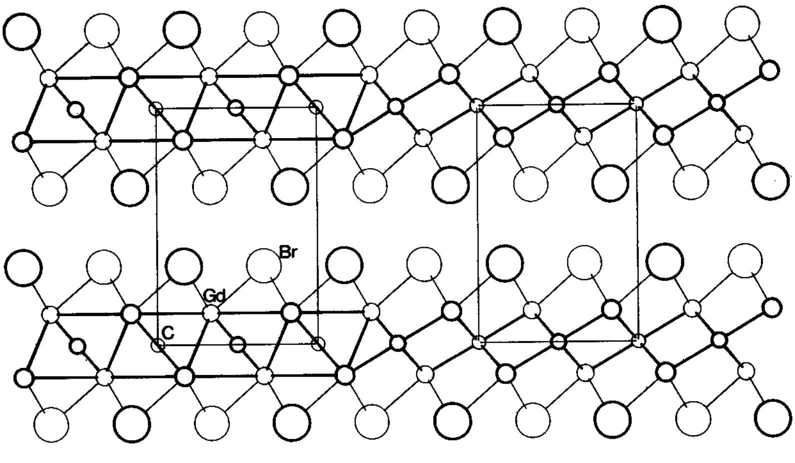

FIG. 3. Projection of the structure of Gd_2Br_2C onto (11.0). One of the two representations may be preferred according to personal taste (see text).

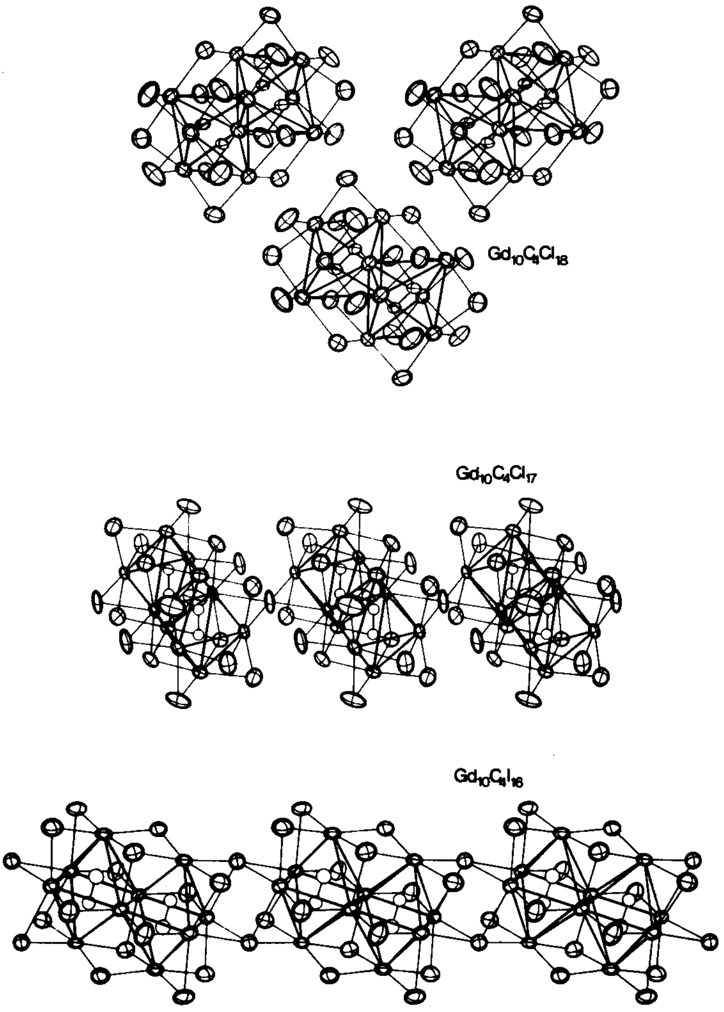

FIG. 4. Projections of representative parts of the structures of $Gd_{10}Cl_{18}C_4$, $Gd_{10}Cl_{17}C_4$, and $Gd_{10}I_{16}C_4$. The edge-sharing Gd_6 octahedra, each centered by C_2 units, are indicated by strong lines. The interconnection of the clusters is shown leading to different stoichiometries.

some back-bonding from carbon π^* levels into empty *d* states. This discussion of chemical bonding in $Gd_{10}Cl_{18}C_4$ is consistent with a band-structure calculation (*68*) which shows that the valence band is filled and well separated from the bottom of the empty *d* band. In the case of $Gd_{10}Cl_{17}C_4$ and $Gd_{10}I_{16}C_4$ the additional 0.5 or 1 electron per C_2 unit, respectively, obviously enter the metal *d* band according to the observation of a constant C–C bond length now leading to classical metal–metal bonds. Obviously the simple balance of electrons which are transferred from the framework to the C_2 unit only holds when each carbon (bonding or antibonding) state can be fully occupied. In the case of the directly comparable pair $Gd_{10}Cl_{18}C_4$ and $Gd_{10}Cl_{17}C_4$ the electronic situation is rather clearly reflected in the interatomic distances (*56*). Whereas the C–C distances are constant, the Gd–Gd distances are up to 9 pm shorter in $Gd_{10}Cl_{17}C_4$. It is also interesting to note that in the case of 7 electrons per C_2 unit ($Gd_{10}I_{16}C_4$) a differentiation into single C atoms and singly bonded C_2 units, although possible, obviously does not take place.

$Gd_6Br_7C_2$ (*57, 61*) can be prepared in good yields from Gd and $GdBr_3$ in the presence of graphite. It forms black needles and according to a single-crystal investigation contains the characteristic double-chain structure described for Tb_6Br_7 (*47*). As one would expect from the electronic balance (18 − 7 = 11 per C_2 unit) single C atoms occupy the octahedral centers. The *Ln*/Br framework is identical within standard deviations for $Gd_6Br_7C_2$ and Tb_6Br_7. Most probably the low-yield binary compound described as Tb_6Br_7 rather represents a ternary phase. A reinvestigation of the original data sets of Tb_6Br_7 and Er_6I_7 reveals electron density near the centers of the Ln_6 octahedra as it is often found with compounds derived from the Ln_6X_{12}-type cluster. The agreement factors become only slightly better, when carbon atoms are introduced in Tb_6Br_7 (R = 0.110 to 0.108) or Er_6I_7 (with $Er_6I_7C_{15}$ changes R = 0.069 to 0.066), although the difference is not as significant as in the case of $Gd_6Br_7C_2$. Further investigations are needed to clarify whether these metal-rich halides exist as binary compounds or need stabilization as ternary phases.

Rather preliminary experiments with other nonmetals than carbon revealed the existence of a new gadolinium chloride nitride.

Gd_2Cl_3N forms grayish needles from reactions of Gd, $GdCl_3$, and N_2 or GdN and $GdCl_3$, respectively. It crystallizes in space group *Pbcn* with a = 1301.7, b = 673.1, and c = 614.0 pm. The structure consists of parallel chains of elongated *trans*-edge-sharing Gd tetrahedra along the c axis (Fig. 5), each one centered by a nitrogen atom. The occurrence of single N atoms is expected. N_2 units (pernitride!) should not occur in metal-rich lanthanide compounds as all electrons offered from the *Ln*/*X* framework only could enter antibonding states in the N_2 unit.

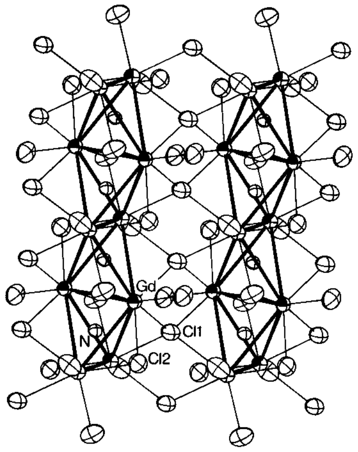

FIG. 5. Structural units of *trans*-edge-sharing Gd_4 tetrahedra, centered by N atoms, in Gd_2Cl_3N. As discussed in the text, the strong lines between Gd atoms do not indicate bonds.

It is interesting to compare the structures of Gd_2Cl_3 (*43, 45*) and Gd_2Cl_3N. The binary chloride contains chains of empty *trans*-edge-sharing Gd octahedra. In a formal way the $NGd_{4/2}$ chains in Gd_2Cl_3N are derived by introducing two N atoms per octahedron, and tetrahedra then form by drastic elongation of the octahedra along the chain direction. In terms of chemical bonding all metal–metal bonding in the chains of octahedra in Gd_2Cl_3 is removed and replaced by strong Gd–N bonding in the tetrahedra of Gd_2Cl_3N. However, the metal–metal distances do not reflect this essential difference in chemical bonding. The Gd–Gd distances belonging to the shared edges are 337 pm in Gd_2Cl_3 and 335 pm in Gd_2Cl_3N, the nonshared edges are 373, 378, and 390 pm in Gd_2Cl_3 and 383, 386, and 397 ppm in Gd_2Cl_3N. This comparison clearly points out the difficulty of deriving metal–metal bond orders from distances (*45, 69*) especially with electropositive metals.

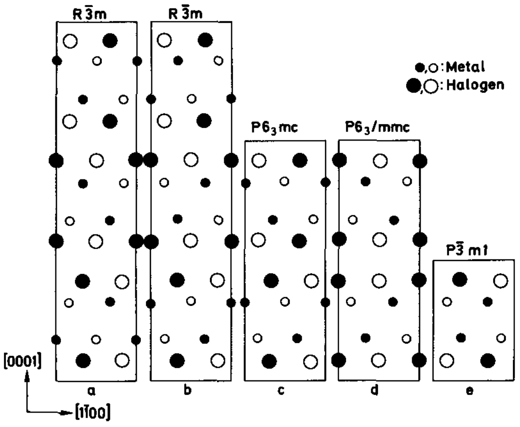

FIG. 6. Heavy-atom arrangements in different types of layered structures. (a) ZrCl, (b) ZrBr, (c) (2s-)$GdBrH_{0.7}$, (d) $M_{0.1}$ YClO, (e) Gd_2Br_2C.

With the ternary lanthanide compounds discussed so far a reversible introduction and removal of the interstitial nonmetal atoms is not possible. A candidate for an intercalations chemistry is hydrogen.

Recent results with Nb_6I_{11} and HNb_6I_{11} helped to open the field of lanthanide halide hydrides. According to earlier experiments, the removal of hydrogen from HNb_6I_{11} is not possible by heating the compound under vacuum, because gaseous NbI_4 is formed before H_2 is released. This decomposition reaction is avoided by heating the compound in a sealed tantalum container which allows only the hydrogen to penetrate, leaving pure Nb_6I_{11} as the residue (*70*). Such a procedure offered a way to overcome the difficulties in the preparation of lanthanide monohalides by first preparing hydrogen-stabilized phases which are then heated to loosen H_2.

By reacting lanthanide trihalides with their respective metals the compounds were isolated in low yields as graphite-like crystals which exhibit an analytically determined metal-to-halogen ratio 1 : 1 and are isotypic with ZrCl or ZrBr (*46*). Many experiments were performed to reach quantitative yields and to grow single crystals. After all, quantitative yields were not attainable with the lanthanides as well as yttrium (*71*) and scandium (*72*), too. This failure could be explained as due to kinetic reasons which do not allow reactions to proceed completely or as due to thermodynamic reasons such as a critically limited temperature range for stability or the necessary stabilization of the phases by impurities.

$GdXH_n$ (X = Cl, Br, I) (*73*). The compounds $GdClH_{0.9}$ and $GdBrH_{0.9}$ can be easily prepared in quantitative yields by heating GdH_2 and the corresponding trihalides in sealed tantalum containers to 900°C. They form black layered crystals with heavy-atom arrangements as in ZrBr (h-GdCl) and ZrCl (t-GdBr). Besides these structures which both represent different stackings of the same kind of XGdHGdX slabs with a repeat distance of three slabs, another stacking variant is found with $GdBrH_{0.7}$ showing a repeat distance of two slabs (2s) (Fig. 6). Adjacent slabs are packed in a way to yield a trigonal-antiprismatic arrangement of the Br atoms. This arrangement corresponds to the anion packing in 2s-NbS_2 and is distinctly different to the very peculiar packing in the two-slab structure of $M_{0.1}$YC10 which exhibits trigonal-prismatic voids between adjacent slabs (*62*) (Fig. 6). This packing is obviously due to the presence of both alkali metal M as well as oxygen (in tetrahedral voids between the layers of Y atoms). The trigonal prismatic packing of Cl atoms might be electrostatically favorable because two O atoms are added to the coordination sphere of the M atoms.

Purposely adding hydrogen to the Gd/GdI_3 system leads to a heterogeneous product of a composition $GdIH_{0.8}$ which contains crystals with a heavy-atom arrangement as in ZrCl but also crystals which are isotypic with the two-slab structure of $GdBrH_{0.7}$. Crystals corresponding to ZrBr could also once be isolated. These

TABLE II

GADOLINIUM HALIDE HYDRIDES (*73*, *80*)

Related Compound	Space group	Lattice constants [pm]		Structure type	Related to
$GdClH_{0.9}$	$R\bar{3}m$	382.4	2749.4	ZrBr	M_6X_8
$GdBrH_{0.8}$	$R\bar{3}m$	387.4	2908.5	ZrCl	M_6X_8
$GdBrH_{0.7}$	$R\bar{3}m$	386.9	2915.0	ZrCl	M_6X_8
$GdBrH_{0.7}$	$P6_3mc$	387.1	1946.3	2s-NbS_2	M_6X_8
$GdIH_{0.8}$	$R\bar{3}m$	398.2	3132.6	ZrBr	M_6X_8
$GdIH_{0.8}$	$R\bar{3}m$	? 392.0	3100.3 ?	ZrCl	M_6X_8
$GdIH_{0.8}$	$P6_3mc$	398.3	2083.2	2s-NbS_2	M_6X_8
$GdBrH_2$	$R\bar{3}m$	381.9	3100.3		M_6X_{12}

results are surprising as earlier systematic search for GdI did not produce any of these phases.

All hydride halides described so far can formally be derived from an edge condensation of Gd_6 octahedra, and the halogen atoms take positions above opposite free faces as in the M_6X_8 cluster. The different positions of the halogen atoms in lanthanide halide carbides (M_6X_{12}) and halide hydrides (M_6X_8) is now easily explained in terms of electrostatic repulsion between X^- and C_n^{m-} and H^-, respectively. Neutron diffraction with $TbClD_{0.8}$ clearly indicates the occupation of the tetrahedral voids between the close-packed layers of Tb atoms (*74*). Therefore, the halogen atoms avoid positions above the occupied tetrahedral voids with the hydrides and avoid positions above the occupied octahedral voids with the carbides. The preference of tetrahedral against octahedral voids with $TbClD_{0.8}$ is the same as with zirconium halide hydrides (*75–78*) and also TbD_2 (*79*), but it does not lead to any recognizable deviation from the trigonal symmetry as in the case of the zirconium compounds.

The range of homogeneity of the compounds $GdXH_n$ or, more generally, MXH_n (M = Sc, Y, La, Ln) is of crucial importance to decide, whether the described monohalides of the trivalent metals are true binary compounds. Heating $GdClH_{0.9}$ or $GdBrH_{0.9}$ in evacuated, electron-beam-welded tantalum containers under vacuum at temperatures below 800°C leads to a slight loss of hydrogen and the formation of homogeneous phases $GdXH_{0.6}$ (*73*). At higher temperatures gadolinium is found in the residues. The total decomposition of $GdXH_n$ into Gd and GdX_3 upon withdrawal of hydrogen could not be demonstrated yet. But our preliminary results seem to indicate that monohalides of the lanthanides are not stable as pure binary compounds.

Experiments to determine the upper phase boundary of $GdBrH_n$ lead to an interesting result (*80*). When $GdBrH_{0.8}$ is heated in H_2 to 400°C it looses its metallic properties and becomes a greenish transparent solid of composition $GdBrH_2$ (analytically $GdBrH_{1.95}$). Heating of the salt $GdBrH_2$ to 680°C at 10^{-6} mbar results in graphite-like $GdBrH_{0.8}$ again. This reaction is accompanied by a shift of all Br atoms from their positions above octahedral faces in $GdBrH_{0.8}$ (M_6X_8) to positions above octahedral edges in $GdBrH_2$ (M_6X_{12}). Whereas the distances within the layers, Gd–Gd = Br–Br = 387 pm as well as the Gd–Br distances (289 pm) and the Br–Br distances between adjacent layers (399 pm) in $GdBrH_{0.8}$ change only slightly, when $GdBrH_2$ is formed (382, 290, and 393 pm, respectively), the most pronounced effect occurs with the interlayer Gd–Gd distances, which change from 355 to 396 pm. Obviously the octahedral voids between the metal layers are also occupied in $GdBrH_2$. But occupation of these voids by single H atoms would only result in a composition $GdBrH_{1.5}$. A neutron diffraction study of $GdBrD_2$ is in progress.

Intermediates between Salts and Metals—Alkali-Metal Suboxides

Lanthanide halide carbides, nitrides, and hydrides represent the borderline between metal–metal-bonded (condensed) cluster compounds and normal valence compounds with highly ionic character.

$Gd_{10}Cl_{18}C_4$, Gd_2Cl_3N, and $GdBrH_2$ are transparent compounds, where all charges of the cations are compensated by the charges of the anions according to formulations as $Gd_{10}^{3+}Cl_{18}^{-}(C_2^{6-})_2$, $Gd_2^{3+}Cl_3^{-}N^{3-}$, or $Gd^{3+}Cl^{-}H_2^{-}$. Metal–metal bonding only comes into play with those compounds which have additional metal valence electrons available, like $Gd_{10}Cl_{17}C_4 = Gd_{10}^{3+}Cl_{17}^{-}(C_2^{6-})_2$ (e^-), $Gd_{10}I_{16}C_4 = Gd_{10}^{3+}I_{16}^{-}(C_2^{6-})_2$ $(2e^-)$, $Gd_{12}I_{17}C_6 = Gd_{12}^{3+}I_{17}^{-}(C_2^{6-})_3$ (e^-) or $GdClH_{0.8} = Gd^{3+}Cl^{-}H_{0.8}^{-}$ $(1.2e^-)$.

The lanthanides are capable of forming compounds with condensed empty clusters as in Gd_2Cl_3, where metal–metal bonding obviously is a structure-determining factor. Frequently, however, clusters of these valence electron poor metals are stabilized by insertion of nonmetal atoms into the cavities inside the clusters and it is rather arbitrary to discuss these structures in terms of stabilized clusters or just to talk about ionic structures which are characterized by the occupation of the voids around the highly charged anions by the cations.

It is fascinating to extrapolate these ideas to the still more valence-electron-poor alkali metals. Recently cluster compounds of alkali metals identified in the gas phase led to some excitement. Molecules like Li_5C, Li_6C, or Li_4O were discussed in terms of hypervalency of carbon or oxygen (*81–83*). The octet rule seems violated, but only if bonding in these molecules is visualized in a very classical way by drawing lines from the central nonmetal to the surrounding (hydrogen-like) Li atoms. Considering, however, the electropositive character of lithium, a description of chemical bonding according to $Li_5^+C^{4-}$ (e^-) or $Li_6^+C^{4-}$ $(2e^-)$ is adequate. The Li cations gather around the central anion—one should not dispute about its actual charge—and there are still electrons left for weak metal–metal bonding besides strong metal–nonmetal bonding. The oxygen-containing clusters like Na_3O or Na_4O might even be more suited for such a description in terms of heteropolar bonding which does not violate the octet rule. A term "hypermetalated" (*84*) or simply metal-rich is adequate rather than "hypervalent" to characterize these molecules.

The "curious suboxides" (*85*) of the heavy alkali metals rubidium and cesium provide a possibility to investigate such clusters in the solid state and characterize them structurally. It is not the purpose of this article to recapitulate details on these compounds described elsewhere (*85–91*) but to draw attention to their existence and to discuss them briefly along the lines presented in the preceding sections.

The rubidium suboxides contain Rb_9O_2 and the cesium suboxides $Cs_{11}O_3$ clusters which are formed by 2 or 3 face-shared metal octahedra, respectively, with an oxygen atom inside each octahedron (Fig. 7). These clusters occur as such or together with stoichiometric amounts of additional alkali metal in Rb_9O_2, $Cs_{11}O_3$, and $Rb_9O_2Rb_x$ $(x = 3)$, $Cs_{11}O_3Rb_y$ $(y = 1, 2, 7)$, $Cs_{11}O_3Cs_z$ $(z = 1, 7)$. The description of chemical bonding in the clusters in terms of a balance of electrons leads to a simple model. According to the formulation $Rb_9^+O_2^{2-}$ $(5e^-)$ and $Cs_{11}^+O_3^{2-}$ $(5e^-)$ the strong metal–nonmetal bonding is assisted by comparatively weak metal–metal bonding, much in the same way as in the earlier mentioned gaseous alkali-metal cluster species. It can be shown, however, that the additional electrons are essential for the stability of the

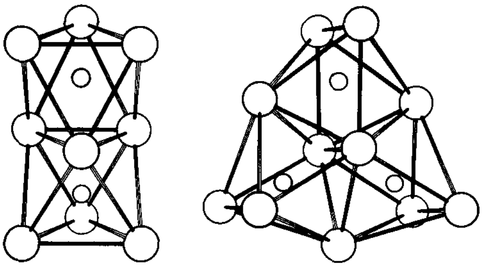

FIG. 7. Rb_9O_2 and $Cs_{11}O_3$ clusters (small circles are O atoms) in alkali-metal suboxides.

clusters (*87*). Lack of the "constriction" (or shielding of the positive charges) due to these additional electrons has the consequence that cations are expelled from the clusters. Both metal–nonmetal bonds as well as metal–metal bonds are necessary for the existence of the clusters in alkalimetal suboxides.

One clearly realizes connections between extremes: Nb_6I_{11} is provided with a sufficiently large number of metal valence electrons for strong metal–metal bonding and for the bonding of external nonmetal atoms. The Nb_6I_8 cluster is able to incorporate the nonmetal atom H into its cavity, but can live without it too. On the contrary, the number of metal valence electrons in $Cs_{11}O_3$ is very small. There is no chance of binding nonmetal atoms externally to the $Cs_{11}O_3$ cluster and the insertion of the nonmetal atoms into the cavities is more essential than the metal–metal bonds for cluster stability. The lanthanide cluster compounds are lying between these extremes.

Much seems to be understood, but more waits to be explained. A Ce(IV) compound might serve as a special example. The structure of $Ce_6(OH)_4(SO_4)_6$ contains M_6X_8 units (*92*). Why?

Acknowledgments

My thanks are due to U. Schwanitz for his help with the figures. The support of Verband der chemischen Industrie—Fonds der Chemie—is gratefully acknowledged.

References

1. F. A. Cotton and F. R. Walton, "Multiple Bonds between Metal Atoms," Wiley, Chichester (1982).

2. Ø. Fischer, *Appl. Phys.* **16,** 1 (1978).

3. D. M. Washecheck, E. W. Wucherer, L. F. Dahl, A Ceriotti, G. Longoni, M. Manassero, M. Sansoni, and P. Chini, *J. Amer. Chem. Soc.* **101,** 6110 (1979).

4. A. Ceriotti, P. Chini, G. Longoni, M. Marchionna, L. F. Dahl, R. Montag, and D. M. Washecheck, *Proc. 15th Congr. Naz. Chim. Inorg.* 93 (1982).

5. G. Schmid, R. Pfeil, R. Boese, F. Brandermann, S. Meyer, G. H. M. Calis, and J. W. A. van der Velden, *Chem. Ber.* **114,** 3634 (1981).

6. J. D. Corbett, *Acc. Chem. Res.* **14,** 239 (1981).

7. A. Simon, *Angew. Chem.* **93,** 23 (1981); *Angew. Chem. Int. Ed. Engl.* **20,** 1 (1981).

8. R. E. McCarley, *Philos. Trans. R. Soc. London Ser. A* **308,** 141 (1982).

9. D. W. Bullett, *Inorg. Chem.* **19,** 1780 (1980).

10. H. Nohl, W. Klose, and O. K. Andersen, *in* "Superconductivity in Ternary Compounds" (Ø. Fischer and M. B. Maple, Eds.), Chap. 6, p. 165, Springer-Verlag, Berlin/Heidelberg (1982).

11. T. Hughbanks and R. Hoffmann, *Inorg. Chem.* **21,** 3578 (1982).

12. T. Hughbanks and R. Hoffmann, *J. Amer. Chem. Soc.* **105,** 1150 (1983).

13. T. Hughbanks and R. Hoffmann, *J. Amer. Chem. Soc.* **105,** 3528 (1983).

14. P. J. Kelly and O. K. Andersen, "Superconductivity in *d*- and *f*-Band Metals," Proceedings, IV Conference, p. 137, Plenum, Karlsruhe/New York (1983).

15. O. K. Andersen and S. Satpathy, *in* "Basic Properties of Binary Oxides" (A. Dominguez Rodriguez, J. Cataing, and R. Marquez, Eds.), p. 21, University of Seville, Spain (1983).

16. J. K. Burdett and T. Hughbanks, *J. Amer. Chem. Soc.* **106,** 3101 (1984).

17. V. Kumar and V. Heine, *J. Phys. F* **14,** 365 (1984); *Inorg. Chem.* **23,** 1498 (1984).

18. F. Dübler and H. Müller, *Wiss. Z. Friedrich-Schiller-Univ. Jena, Math.-Naturwiss. Rehie* **31,** 907 (1982).

19. L. R. Bateman, J. F. Blount, and L. F. Dahl, *J. Amer. Chem. Soc.* **88,** 1082 (1982).

20. A. Simon, H. G. v. Schnering, and H. Schäfer, *Z. Anorg. Allg. Chem.* **355,** 295 (1967).

21. A. Simon, *Z. Anorg. Allg. Chem.* **355,** 311 (1967).

22. H. Nohl and O. K. Andersen, *Conf. Ser. Inst. Phys.* **55,** 61 (1980).

23. J. J. Finley, H. Nohl, E. E. Vogel, H. Imoto, R. E. Camley, V. Zevin, O. K. Andersen, and A. Simon, *Phys. Rev. Lett.* **46,** 1472 (1981).

24. J. J. Finley, R. E. Camley, E. E. Vogel, V. Zevin, and E. Gmelin, *Phys. Rev. B* **24,** 1323 (1981).

25. H. Imoto and A. Simon, *Inorg. Chem.* **21,** 308 (1982).

26. F. Dübler, H. Müller, and Ch. Opitz, *Chem. Phys. Lett.* **88,** 467 (1982).

27. F. Stollmaier and A. Simon, *Inorg. Chem.,* in press.

28. W. Bronger, H.-J. Miessen, P. Müller, and R. Neuröschel, *J. Less-Common Met.*, in press.
29. H. Imoto and J. D. Corbett, *Inorg. Chem.* **19,** 1241 (1980).
30. W. J. Westerhaus, H. Imoto, E. Warkentin, and A. Simon, to be published.
31. H. Imoto and A. Simon, *in* A. Simon, *Ann. Chim. Fr.* **7,** 539 (1982).
32. A. N. Fitch, S.-A. Barrett, and B. E. F. Fender, *J. Chem. Soc. Dalton Trans.*, 501 (1984).
33. D. E. Eastman, J. K. Cashion, and A. C. Switendick, *Phys. Rev. Lett.* **27,** 35 (1971).
34. O. Jepsen, R. M. Nieminen, and J. Madsen, *Solid State Commun.* **34,** 575 (1980).
35. H. Bilz, *Z. Phys.* **153,** 338 (1958).
36. S. Wijeyesekera and R. Hoffman, *Organometallics*, in press.
37. H. G. V. Schnering, unpublished remark (1982).
38. H. Schäfer and H. G. Schnering, *Angew. Chem.* **76,** 833 (1964).
39. H. Nohl and O. K. Andersen, to be published (see (*31*)).
40. R. Chevrel, *J. Solid State Chem.*, in press.
41. H.-Y. Chen and H. F. Franzen, *Nat. Bur. Stand. (U.S.) Spec. Publ.* **364,** 651 (1972).
42. H. F. Franzen, *Prog. Solid State Chem.* **12,** 1 (1978).
43. D. A. Lokken and J. D. Corbett, *Inorg. Chem.* **12,** 556 (1973).
44. A. Simon, HJ. Mattausch, and N. Holzer, *Angew. Chem.* **88,** 685 (1976); *Angew. Chem. Int. Ed. Engl.* **15,** 624 (1976).
45. A. Simon, N. Holzer, and HJ. Mattausch, *Z. Anorg. Allg. Chem.* **456,** 207 (1979).
46. HJ. Mattausch, A. Simon, N. Holzer, and R. Eger, *Z. Anorg. Allg. Chem.* **466,** 7 (1980).
47. K. Berroth, HJ. Mattausch, and A. Simon, *Z. Naturforsch. B* **35,** 626 (1980).
48. K. Berroth and A. Simon, *J. Less-Common Met.* **76,** 41 (1980).
49. R. E. Aranjo and J. D. Corbett, *Inorg. Chem.* **20,** 3082 (1981).
50. A. Simon, *in* "Crystalline Electric Field Effects in f-Electron Magnetism" (R. P. Guertin, W. Suski, and Z. Zolnierek, Eds.), p. 443, Plenum, New York (1982).
51. G. Ebbinghaus, A. Simon, and A. Griffiths, *Z. Naturforsch. A* **37,** 564 (1982).
52. W.. Bauhofer and A. Simon, *Z. Naturforsch. A* **37,** 568 (1982).
53. A. Simon, *J. Less-Common Met.* **93,** 369 (1983).
54. A. Simon, *Naturwissenschaften* **71,** 171 (1984).
55. A. Simon, E. Warkentin, and R. Masse, *Angew. Chem.* **93,** 1071 (1981); *Angew. Chem. Int. Ed.* **20,** 1013 (1981).
56. E. Warkentin, R. Masse, and A. Simon, *Z. Anorg. Allg. Chem.* **491,** 323 (1982).
57. U. Schwanitz and A. Simon, *Z. Naturforsch. B*, in press.
58. A. Simon and E. Warkentin, *Z. Anorg. Allg. Chem.* **497** 79 (1983).
59. A. Simon and E. Warkentin, in press.
60. E. Warkentin and A. Simon, *Rev. Chim. Miner.* **20,** 488 (1983).
61. U. Schwanitz, thesis, Stuttgart (1984).
62. J. E. Ford, J. D. Corbett, and S.-J. Hwu, *Inorg. Chem.* **22,** 2789 (1983).
63. D. G. Adolphson and J. D. Corbett, *Inorg. Chem.* **15,** 1820 (1976).
64. R. L. Daake and J. D. Corbett, *Inorg. Chem.* **16,** 2029 (1977).
65. E. A. Turow, "Physical Properties of Magnetically Ordered Crystals," p. 80, Academic Press, New York (1965).
66. A. Kjekshus, *Acta Chem. Scand.* **18,** 2379 (1964).
67. C. M. T. Hayward, J. R. Shapley, M. R. Churchill, C. Bueno, and A. L. Rheingold, *J. Amer. Chem. Soc.* **104,** 7347 (1982).
68. S. Satpathy, to be published.
69. J. D. Corbett, *J. Solid State Chem.* **37,** 335 (1981).
70. F. Stollmaier and A. Simon, unpublished results (1984).
71. HJ. Mattausch, J. B. Hendricks, R. Eger, J. D. Corbett, and A. Simon, *Inorg. Chem.* **19,** 2128 (1980).
72. K. R. Poeppelmeier and J. D. Corbett, *Inorg. Chem.* **16,** 294 (1977).
73. HJ. Mattausch, W. Schramm, A. Simon, and R. Eger, *Z. Anorg. Allg. Chem.*, in press.
74. F. Ueno, K. Ziebeck, HJ. Mattausch, and A. Simon, *Rev. Chim. Miner.*, in press.
75. H. S. Marek, J. D. Corbett, and R. L. Daake, *J. Less-Common Met.* **89,** 243 (1983).
76. T. Y. Hwang, D. R. Torgeson, and R. G. Barnes, *Phys. Lett. A* **66A,** 137 (1978).
77. P. Dubois Murphy and B. C. Gerstein, *J. Chem. Phys.* **70,** 4552 (1979).
78. T. Y. Hwang, R. J. Schönberger, D. R. Torgeson, and R. G. Barnes, *Phys. Rev. B* **27,** 27 (1983).
79. D. E. Cox, G. Shirane, W. J. Takei, and W. E. Wallace, *J. Appl. Phys.* **34,** 1352 (1963).
80. A. Simon, HJ. Mattausch, and R. Eger, to be published.
81. P. V. R. Schleyer, E.-U. Würthwein, and J. A. Pople, *J. Amer. Chem. Soc.* **104,** 5839 (1982).
82. P. V. R. Schleyer, E.-U. Würthwein, E. Kaufmann, T. Clark, and J. A. Pople, *J. Amer. Chem. Soc.* **105,** 5930 (1983).
83. P. V. R. Schleyer, *in* "New Horizons of Quan-

tum Chemistry" (P.-O. Löwdin and B. Pullmann, Eds.), p. 95, Reidel, Dordrecht (1983).

84. E.-U. WÜRTHWEIN, P. V. R. SCHLEYER, AND J. A. POPLE, *J. Amer. Chem. Soc.*, in press.

85. F. A. COTTON AND G. WILKINSON, "Advanced Inorganic Chemistry," 4th ed., p. 254, Wiley, New York (1980).

86. A. SIMON, *in* "Structure and Bonding" (J. D. Dunitz *et al.,* Eds.), Vol. 36, p. 81, Springer-Verlag, Berlin/Heidelberg (1979).

87. T. P. MARTIN, H.-J. STOLZ, G. EBBINGHAUS, AND A. SIMON, *J. Chem. Phys.* **70,** 1096 (1979).

88. G. EBBINGHAUS AND A. SIMON, *Chem. Phys.* **43,** 117 (1980).

89. H.-J. DEISEROTH AND A. SIMON, *Z. Anorg. Allg. Chem.* **463,** 14 (1980).

90. E. GMELIN, A. SIMON, W. BRÄMER, AND R. VILLAR, *J. Chem. Phys.* **76,** 6256 (1982).

91. H.-J. DEISEROTH AND A. SIMON, *Rev. Chim. Miner.* **20,** 475 (1983).

92. G. LUNDGREN, *Ark. Kemi* **10,** 183 (1956).